Rickels, Wilfried; Lontzek, Thomas S.

Working Paper

Optimal global carbon management with ocean sequestration

Kiel Working Paper, No. 1432

Provided in Cooperation with:
Kiel Institute for the World Economy – Leibniz Center for Research on Global Economic Challenges

Suggested Citation: Rickels, Wilfried; Lontzek, Thomas S. (2008) : Optimal global carbon management with ocean sequestration, Kiel Working Paper, No. 1432, Kiel Institute for the World Economy (IfW), Kiel

This Version is available at:
https://hdl.handle.net/10419/4316

Kiel Working Papers

Kiel Institute for the World Economy

Optimal Global Carbon Management with Ocean Sequestration

by Wilfried Rickels and Thomas Lontzek

No. 1432 | July 2008

Web: www.ifw-kiel.de

Kiel Working Paper No. 1342 | July 2008

Optimal Global Carbon Management with Ocean Sequestration

Wilfried Rickels and Thomas Lontzek

We investigate the socially optimal anthropogenic intervention into the global carbon cycle. The limiting factor for this intervention is the accumulation of carbon in the atmosphere, which causes global warming. We apply a simplified two-box model to incorporate aspects of the global carbon cycle in a more appropriate way than a simple proportional decay assumption does. Anthropogenic intervention into the global carbon cycle enters the model as the amount of CO2 emitted into the atmosphere and the amount of CO2 injected into the deep ocean for purposes of sequestration. We derive a critical cost level for sequestration above which sequestration is just a temporary option or below which it is the long-run option allowing extended use of fossil fuels. The second option involves higher atmospheric stabilization levels, whereby the efficiency of sequestration depends on the time preference and the inertia of the carbon cycle.

Keywords: Climate Change, Global Carbon Cycle, CO2 Emissions, Sequestration

JEL classification: Q30; Q54

Wilfried Rickels
Kiel Institute for the World Economy
24100 Kiel, Germany
Telephone: +49 431 8814408
E-mail: wilfried.rickels@ifw-kiel.de

Thomas Lontzek
Kiel Institute for the World Economy
24100 Kiel, Germany
Telephone:+ 49 431 8814 405
E-mail: thomas.lontzek@ifw-kiel.de

Optimal Global Carbon Management with Ocean Sequestration *

Wilfried Rickels† , Thomas Lontzek‡

Abstract

We investigate the socially optimal anthropogenic intervention into the global carbon cycle. The limiting factor for this intervention is the accumulation of carbon in the atmosphere, which causes global warming. We apply a simplified two-box model to incorporate aspects of the global carbon cycle in a more appropriate way than a simple proportional decay assumption does. Anthropogenic intervention into the global carbon cycle enters the model as the amount of CO_2 emitted into the atmosphere and the amount of CO_2 injected into the deep ocean for purposes of sequestration. We derive a critical cost level for sequestration above which sequestration is just a temporary option or below which it is the long-run option allowing extended use of fossil fuels. The second option involves higher atmospheric stabilization levels, whereby the efficiency of sequestration depends on the time preference and the inertia of the carbon cycle.

JEL Classification: Q30; Q54

Keywords: Climate Change, Global Carbon Cycle, CO_2 Emissions, Sequestration

*This work was done as part of the ongoing interdisciplinary research within the Future Ocean cluster of excellence, which also provided financial support for Wilfried Rickels. We would like to thank Andreas Oschlies, Toste Tanhua, Till Requate and Martin Quaas for helpful comments and suggestions. The usual caveats apply.

†Corresponding author. Kiel Institute for the World Economy, Düsternbrooker Weg 120, 24105, Kiel, Germany. Phone: +49 431 8814 408. Email: Wilfried.Rickels@ifw-kiel.de

‡Kiel Institute for the World Economy. Email: Thomas.Lontzek@ifw-kiel.de

1 Introduction

Today, society has recognized the far-reaching consequences of the increase in carbon in atmosphere to above its preindustrial level because this contributes to a large extent to global warming. Nevertheless, the carbon stock in the atmosphere is growing continuously and its growth rate increased even further in the period 2000-2006. (Canadell et al. [1]). This growth depends not only on global economic activity and the carbon intensity of the economy but also on the effectiveness of the natural carbon sinks, the terrestrial biosphere and the ocean. The change in atmospheric carbon in a given year relative to that year's total carbon emissions constitutes the airborne fraction (AF) of carbon. This ratio is currently substantially lower than 1, which indicates that the natural sinks are removing anthropogenic carbon from the atmosphere. Canadell et al. [1] estimate the AF to be 0.45 for the period 2000 to 2006, whereby the ocean sink removed around 0.25 and natural sinks on land removed around 0.3. But the uptake by the land sinks is subject to strong fluctuations that are not well understood yet. Looking at the change in the various carbon reservoirs from 1800 to 1994, Sabine et al. [11] show that the terrestrial biosphere has been a total net source of 39 ($\pm$28) Gt C.[1] They conclude that "the ocean has constituted the only true net sink for anthropogenic CO_2 over the past 200 years "(p.370). The absolute value of the long-run atmospheric carbon stabilization level and the time pattern of its achievement will depend crucially on the marine carbon cycle, which is therefore perceived to be the most import cycle with regard to the climate (Najjar [10]). Therefore, any approach to manage the global carbon cycle or to mitigate global warming that ignores the ocean ignores optimization potential.

Many optimal control models that are used to determine the optimal carbon tax in a climate change setting apply a constant rate of decay, which yields a proportional decay of carbon in the atmosphere. As a result, in these models, global warming presents itself merely as a problem of temporary duration because the stock of carbon in the atmosphere returns to its preindustrial level when fossil fuel reserves are limited (see, e.g., Tahvonen [14]). Such models, however, only roughly approximate the global carbon cycle. In reality this "decay" is not really a decay per se, but rather the shifting of carbon from the atmosphere to the other carbon reservoirs. Hence, it simply cannot be captured by a constant rate, which implies that the atmosphere is a completely renewable resource. In this paper, we address the question how the inclusion of the largest carbon reservoir of the carbon cycle, the ocean, changes the optimal path of carbon emissions and whether its inclusion allows additional optimization potential.

[1]Based on the net increase of 165 Gt carbon in the atmosphere from 1800 to 1994, [11] subtract their ocean inventory estimate of 118 ($\pm$ 19) Gt carbon from the total of fossil-fuel-emitted carbon, which amounted to 244($\pm$20) Gt during this period. As a consequence, the terrestrial biosphere has to be considered a net source of carbon if the carbon budget is to be balanced.

Variations in the transfer rates between the various reservoirs in the carbon cycle due to differences in their relative carbon stock sizes are investigated to some extent in the literature on nonconstant pollution decay. Here, the decay rate is a function of the size of the pollution stock. The decay function is concave over some interval, whereby, when the pollution stock exceeds the upper boundary, the natural decay process is destroyed (see, e.g., Forster [5], Tahvonen and Withagen [15], and Toman and Withagen [16]). In general, however, models that assume a nonconstant decay suffer from a major shortcoming in climate change context applications: they are concerned with carbon "decay" in the atmosphere only, whereby, as long as the decay capacity is not exhausted, carbon continues to be removed from the atmosphere. If, in addition, no resource constraint is included, steady states with positive pollution and decay rates can emerge. Farzin and Tahvonen [4] incorporate the nonrenewable aspect of the global carbon cycle to some extent into their model. Based on a paper by Maier-Raimer and Hasselmann [9], they divide the atmospheric stock of carbon within their dynamic system artificially into two different stocks, one with a constant rate of decay and the other without. As a result, the dynamic system converges towards a steady state with a carbon stock above the preindustrial level and zero extraction. Given that the proportion of emissions to the nondecaying stock is equal to the long-run equilibrium, the model of Farzin and Tahvonen [4] captures important aspects of the carbon cycle. Nevertheless, the only management option in their dynamic system is to control the amount of emissions released into the atmosphere, which is proportional to the amount of extracted fossil fuels.

Nowadays, carbon capture and storage (CCS) is considered an additional option for reducing atmospheric CO_2 emissions by unmating the use of fossil fuels and emissions. One of the potential CCS options is to inject CO_2 into the deep ocean (IPCC [7]). Ocean CO_2 storage entails characteristics of both temporary and permanent storage. The upper limit for the amount of permanent storage is determined by the long-run atmosphere-ocean equilibrium. CO_2 injected into the deep ocean in excess of this amount, is expected to leak back to the atmosphere, because the ocean becomes supersaturated in relation to the atmosphere. Herzog et al. [6] calculate the CCS effectiveness of injecting CO_2 into the deep ocean, whereby CCS effectiveness is measured as the ratio between the net benefit gained from temporary storage and the benefit gained from permanent storage. They find " that the value of relatively deep ocean sequestration is nearly equivalent to permanent sequestration if marginal damage (i.e., carbon prices) remains constant or if there is a backstop technology that caps the abatement cost in the not too distant future" (p.306).

In this paper, we apply a two-box model to include the oceanic carbon stock in the stock externality problem of carbon accumulation in the atmosphere due to fossil fuel consumption. Thereby, we replace the constant or nonconstant decay assumption and capture the essential nonrenewable

aspects of the global carbon cycle without artificially dividing the atmospheric carbon stock. Additionally, we introduce ocean sequestration as a control variable to consider its effectiveness not in an isolated manner but as an additional option in a combined extraction and sequestration decision. We show without specifying functional forms that the admissible paths for the emission and sequestration tax are either monotonically increasing or U-shaped. In doing so, we can show that the optimal path of extraction and ocean sequestration does not allow an interior solution. In the constrained optimization problem, we introduce functional forms and derive a critical cost level for sequestration. Below this cost level, ocean sequestration is the long-run option for fossil fuel consumption because the complete amount of emissions is sequestered. When the sequestration costs are equal or greater than the critical cost level, sequestration will never be utilized in the long run. However, it might still serve as a temporary option to adjust for high initial levels of carbon in the atmosphere. The stabilization levels in the atmosphere and the ocean are increasing in the degree that ocean sequestration is utilized. As a consequence, the utilization of ocean sequestration can extend our capabilities of deriving utility from fossil fuel consumption, but will also exacerbate the problem of global warming in the long run.

The paper proceeds as follows. In Section 2 we explain some important facts of the marine carbon cycle and ocean sequestration. These facts demonstrate the necessity of including the marine carbon cycle in any approach for global carbon management, but are not essential for understanding the model. In Section 3 we present our model. In Subsection 3.1 we introduce and explain our model, in Subsection 3.2 we derive the general properties about the path of the emissions taxes, and in Subsection 3.3 we derive the admissible steady states and the dynamic properties of the model. Section 4 concludes.

2 Natural Ocean Uptake and Ocean Storage

The reason that there is a net transfer of carbon between the atmosphere and the ocean is that there is a difference in the partial pressure of carbon dioxide (pCO_2) between these two reservoirs. As long as the partial pressure in the atmosphere is larger than in the ocean, we will observe a net transfer into the ocean. The ocean contains about 65 times more carbon than the atmosphere. This difference is explained not only by the size of these two reservoirs, but also by the chemical reactivity of CO_2 in water and the various carbon pumps in the ocean. Most of the CO_2 dissolves in water, forming carbon acid first and then bicarbonate (HCO_3^-) and carbonate ions (CO_3^{2-}). The sum of these three elements describes the total amount of carbon in the ocean, called dissolved inorganic carbon (DIC). The amount of DIC in the ocean consists to 89.1% of bicarbonate ions, to 10.4% of

carbonate ions and only to 0.5% of CO_2 (Najjar [10]). Regarding the last figure, the atmosphere "sees" only a tiny fraction of the carbon present in ocean surface water within the chemical process of pCO_2 equilibration between the atmosphere and the ocean. The chemical reactivity of CO_2 constitutes a chemical sink for CO_2 in the mixed layer. The effectiveness of this chemical sink can be measured by the buffer factor, which measures, for a given release of CO_2 into the atmosphere, the fractional change in atmospheric CO_2 relative to the fractional change in DIC: $\zeta = \frac{\partial[CO_2]/[CO_2]}{\partial[DIC]/[DIC]}$. A low buffer factor therefore indicates that a large fraction of the atmospheric CO_2 perturbation can be taken up by the ocean. The value of the buffer factor is proportional to the ratio between DIC and alkalinity (Sabine et al. [11]).[2]

The buffer factor measures the ability of the ocean to take up carbon from the atmosphere, but not the speed of this uptake. Compared to the total size of the ocean, only a small fraction of it is in direct exchange with the atmosphere. Whereas the equilibration time for the upper layer of the ocean with the atmosphere takes around one year, the uptake bottleneck is the transport of anthropogenic CO_2 to the deeper parts of the ocean. This transport is effected by the biological pump and the solubility pump. The biological pump is driven by two cycles: the organic matter cycle and the calcium carbonate cycle. Within the first cycle, phytoplankton captures CO_2 through photosynthesis and produces its organic tissue by utilizing the inorganic nutrients that are dissolved in seawater. The reverse process is respiration and mineralization of this organic matter. Whereas photosynthetic production is restricted to the light-lit euphotic zone, remineralization is not and, as a consequence, occurs on average deeper in the water column.[3] The organic matter cycle causes surface depletion and deep enrichment of DIC, but causes slight surface enrichment and deep depletion of alkalinity in the top layer. Therefore, the organic matter pump decreases surface ocean pCO_2 and hence, pCO_2 in the atmosphere (Najjar [10]). The second cycle works in the opposite direction. Its driving forces are plants and animals that build their $CaCO_3$ skeletons in the euphotic zone from dissolved calcium and carbonate ions. When these skeletons sink in the water column, they dissolve back into calcium and carbonate ions. Ocean circulation transports these ions back to the surface layer. This cycle creates a surface depletion and deep enrichment in DIC and alkalinity. The effect of the calcium carbonate cycle on alkalinity is about twice as strong as its effect on DIC. As a consequence, it increases pCO_2 in the upper layer and therefore increases atmospheric CO_2. Both cycles are present mainly in the upper layer of the ocean. The term biological pump designates the

[2] Alkalinity measures the ability of seawater to maintain its pH-value when carbon acids are added. The pH-value determines the distribution of DIC between the three different carbon forms, but is itself affected by the additional uptake of carbon.

[3] The euphotic zone is the layer that receives enough light for photosynthesis to occur. The depth of this layer is determined by the amount of incoming sunlight and the activity of the water (Sarmiento and Gruber [12] p.111). The aphotic zone is the layer below the euphotic zone.

small fraction of organic matter and skeletons that survives remineralization in the euphotic zone and sinks to deeper layers. On the way to the deep ocean, this material is degraded further by microbial processes, so that an even smaller fraction reaches the seafloor. Here, the remineralization process continue, so that only a very small fraction of the carbon is buried. The amount of carbon removed from the global carbon cylce by sedimentary burial is offset mainly by the natural carbon intake through rivers, which transport carbon released through weathering into the ocean.[4] Due to their influence on DIC and alkalinity and hence pCO2, both cycles, the organic matter cycle and the calcium carbonate cycle, are important factors for the chemical equilibration of carbon between the atmosphere and the upper layer of the ocean. For overall equilibration, however, the transport of carbon into the deep ocean is important. This transport is effected by the biological pump and especially by the solubility pump. The solubility pump is driven by two phenomena: thermohaline circulation and the solubility of CO_2. Surface water in equilibrium with atmospheric CO_2 takes up additional CO_2 on its way to the poles, as the decreasing temperature increases the solubility of CO_2. The formation of deep seawater is driven by thermohaline circulation, which transports cold and high-solubility high-latitude surface waters into the deep ocean. Consequently, these two phenomena act together to pump carbon from the atmosphere into the ocean's deeper layers. However, for increasing atmospheric CO2, this uptake process is limited mainly by the turnover speed, and the total ocean will still be undersaturated for a long time (order of 10^3 years) (Körtzinger and Wallace [8]).

Since natural forces transport carbon into the deep ocean, where it cannot affect society as adversely as when in the atmosphere, the logical question is: Why do we not accelerate the process of downward carbon transfer by injecting carbon into the deep ocean? CO_2 could be transported via pipelines or ships to an ocean storage site, where it would be injected into the water column of the ocean or at the seafloor (IPCC [7] p. 37). This way, it would also become part of the global carbon cycle, but would enter the cycle in a more favorable way. The upper limit of storing injected carbon in the ocean depends on the ocean equilibration with the atmosphere. Consequently, the oceanic equilibration value for various stabilization scenarios in the atmosphere would constitute this upper limit. (IPCC [7] p.38).

[4]The organic matter cycle has an annual gross primary production of 103 Gt C. Roughly 90% of this production is repatriated within the euphotic zone. From the remaining 10% only 1% reaches the seafloor, where annually around 0.01 Gt C are buried (Körtzinger and Wallace [8]). The carbon flux produced annually by the calcium carbonate cycle is only 0.4 Gt C, but 50% of this is buried in sediments (Körtzinger and Wallace [8]).

3 Model

3.1 Model Description

The global carbon cycle is represented in our model by a simple two-box model, where both boxes represent carbon stocks. The upper box, S, aggregates the carbon stocks in the atmosphere and in the upper mixed layer of the ocean. We assume that the atmosphere and the upper mixed layer are always in equilibrium and that the stock of carbon in the atmosphere is a constant fraction, s, of the upper box. The lower box, W, is coterminous with the carbon stock in the deep ocean. The upper box is relatively small in comparison to the lower box. There will be a net flux between these two boxes when there is a difference between their relative stock sizes. An increase in the stock size in the upper box causes a downward transfer of excess carbon into the deep ocean, whereas upwelling water is still free of excess carbon, so that we observe a net transfer from the upper box into the lower box. A new equilibrium is established when both boxes contain the same concentration of excess carbon.[5] The anthropogenic disturbance in this model is fossil-fuel-based emissions, $q(t)$ at time t, which are released into the upper box, and the amount of carbon sequestered and injected into the lower box,[6] $a(t)$ at time t. The emissions are proportional to the use of fossil reserves and we choose units so that proportionality is unity. Subtracting the amount of sequestration from the total amount of emissions yields the net emissions into the upper box. The two-box model is described by two equations of motion for the two boxes, which include the proportionality factor ω to scale the stock of carbon in the lower box with respect to the upper box and the factor turnover factor γ, which describes the speed of the adjustment process:[7]

$$\dot{S} = q(t) - a(t) - \gamma(S(t) - \omega W(t)) \quad \text{with} \quad S(t_0) = S_0, \tag{1}$$

$$\dot{W} = a(t) + \gamma(S(t) - \omega W(t)) \quad \text{with} \quad W(t_0) = W_0. \tag{2}$$

We investigate the optimal anthropogenic intervention as social planner's problem, in which he needs to determine the global optimal amounts of extraction and sequestration. The social planner faces an objective function in which gross utility of society at any instant of time is generated by the extraction and use of fossil fuels, $q(t)$. The proportional emissions, $q(t)$, increase the amount

[5] The ocean is by far the largest carbon reservoir in the global carbon cycle and it is estimated that the ocean will take up around 85 % of the anthropogenic CO_2 emissions in the long run (Körtzinger and Wallace [8]). Note that we assume that sedimentary burial is constant and does not depend on the stock of carbon in the ocean and that this amount is balanced by the carbon that is input into the ocean by rivers and volcanos. However, on even longer time scales of thousands of years, this sediment buffer will be enhanced, so that carbon will be removed from the system again.

[6] Note that throughout the paper we denote this activity only as sequestration.

[7] Given our knowledge of the size of the carbon stock in the deep ocean and the low transfer of anthropogenic carbon into the deeper parts of the ocean, we can state without loss of generality that only very small values have to be considered for these two parameters.

of carbon in the two-box model, whereby the increase in the stock of carbon in the atmosphere to above preindustrial levels, $s * S(t) - A_{preind}$, leads to global warming and thereby causes social costs for society at any instant in time. The gross utility of fossil fuel extraction and utilization is described by $U(q(t))$, which has the properties $U' > 0, \quad U'' < 0$, and $U'(0) = b < \infty$. The last property implies that there is a choke price or a backstop price. We assume that the costs of fossil fuel extraction are constant and are included in $U(q(t))$. The social costs of global warming are denoted as damage and are described by the strictly convex function $D(S(t))$, with the properties $D' > 0, \quad D'' > 0$, and $D'(0) = 0$. The equations (1) and (2) indicate that no carbon will vanish from the system[8] and that therefore the release of carbon will increase the stock in both boxes forever. As a result, there will be a new equilibrium where either the fossil reserves are completely extracted or the marginal damage is equal to the backstop price. However, regarding various goals for climate change stabilization, the limiting factor does not seem to be the endowment of fossil reserves, but rather the storing capacity of the atmosphere. We therefore do not include a stock of fossil reserves, which simplifies the analysis and the qualitative results. However, we do include sequestration costs in the objective function. Sequestration costs are described by $A(a(t))$, which is also a convex function with the properties $A' > 0$, and $A'' > 0$, and which are measured in the same units as utility and damage. The objective function for the social planner is

$$\max_{q(t),a(t)} \int_0^\infty (U(q) - A(a(t)) - D(S(t)))e^{-\rho t} dt, \tag{3}$$

$$\text{with} \quad a(t), q(t) \geq 0 \quad \text{and} \quad q(t) - a(t) \geq 0. \tag{4}$$

In the next two sections, we analyze the properties of optimal extraction and sequestration. Our aim is to derive the optimal steering of the carbon cycle from levels similar to the preindustrial case and from levels where the carbon stock in the upper box is already significantly higher than the preindustrial level, while the carbon stock in the lower box is still close to that level.

3.2 General Results

We derive the corresponding current value Hamiltonian from (1), (2), and (3):

$$H_c = U(q) - A(a) - D(S)) - \psi \dot{S} - \pi \dot{W}, \tag{5}$$

$$\text{where} \quad \lim_{t \to \infty} S(t), W(t) \geq 0. \tag{6}$$

[8] On longer time scales of thousands of years, it is assumed that there is sufficient sedimentary $CaCO_3$ available to neutralize all fossil fuel reserves (Najjar [10] p.275).

Note that from now on we drop the time variable whenever it is convenient. We have changed the signs of the costate variables, ψ and π, in order to facilitate their economic interpretation as a tax. Together with the two Lagrange multipliers, θ_1 and θ_2, we obtain the current value Lagrangian:

$$L_c = H_c - \theta_1(a - q) - \theta_2(-a). \tag{7}$$

The necessary first-order conditions (FOC) for the admissible solution candidates that satisfy conditions (1), (2), and (4) are:

$$\begin{aligned}
\frac{\partial L_c}{\partial q} &= 0 \quad \Rightarrow \quad U'(q) - \psi - \theta_1 = 0, && (8)\\
\frac{\partial L_c}{\partial a} &= 0 \quad \Rightarrow \quad -A'(a) + \psi - \pi - \theta_1 + \theta_2 = 0, && (9)\\
-\frac{\partial L_c}{\partial S} &= -\dot{\psi} + \rho\psi \quad \Rightarrow \quad -D'(S) + \gamma\psi - \gamma\pi = \dot{\psi} - \rho\psi, && (10)\\
-\frac{\partial L_c}{\partial W} &= -\dot{\pi} + \rho\pi \quad \Rightarrow \quad -\gamma\omega\psi + \gamma\omega\pi = \dot{\pi} - \rho\pi, && (11)\\
\frac{\partial L_c}{\partial \theta_1} &\geq 0 \quad \theta_1 \geq 0 \quad \theta_1(a - q) = 0, && (12)\\
\frac{\partial L_c}{\partial \theta_2} &\geq 0 \quad \theta_2 \geq 0 \quad \theta_2(-a) = 0. && (13)
\end{aligned}$$

Additionally, we assume that $\lim_{S\to\infty} D(S) < \infty$ and that therefore the integral (3) converges for all admissible pairs of q, a, S, W. The current value Lagrangian for an interior solution reduces to the current value Hamiltonian. Due to Theorem 13 in [13] p. 234, our solution candidate, q^*, a^*, S^*, W^*, is optimal, if conditions (8) to (11) are satisfied, if the Hamiltonian is concave, and if the transversality conditions

$$\lim_{t\to\infty} e^{-\rho t}\psi \geq 0, \quad \lim_{t\to\infty} e^{-\rho t}\pi \geq 0 \tag{14}$$

are fulfilled.[9] As our Hamiltonian is concave, but not strictly concave, we have to identify a unique solution candidate for global optimality. But as we will show later, our dynamic system obeys saddle path properties and that the optimal solution will approach a steady state, this condition is fulfilled.

From the FOCs we can already derive some insights about the dynamic solution properties. As already mentioned, we interpret the costate variables as taxes, whereby the costate variable that corresponds to the carbon stock in the upper box, ψ, has the meaning of an emission tax, and the

[9]Note that in the infinite horizon context the complete transversality conditions for costate variables are: $\lim_{t\to\infty} \psi(S(t) - S^*(t)) \geq 0$ and $\lim_{t\to\infty} \pi(W(t) - W^*(t)) \geq 0$. But as our objective function contains time discounting and we assumed an upper bound below infinity for damage, the integral converges. As a result, we can use the more simple transversality conditions (14) as sufficient conditions. This is also justified by the fact, that the system approaches a steady state. For a discussion about sufficient transversality conditions in an infinite horizon problem, see Chiang [2] pp.240-251 and Theorem 16 in Seierstad and Syssæter [13] p. 244 Equation (214) and Note 22.

costate variable that corresponds to the carbon stock in the lower box, π, has the meaning of a sequestration tax. Through time, the marginal utility of fossil fuel extraction should be equal to the emission tax, ψ. Extraction stops when the emission tax has risen to the value of the choke price. The level of sequestration is determined by the difference between the emission tax and the sequestration tax. The level of the emission tax, ψ, has the opposite effect on the level of extraction and sequestration. The level of ψ indicates the magnitude of the carbon stock problem in the upper box via the damage function. An increasing level of carbon in the upper box corresponds to higher damage. Therefore, it is optimal to decrease emissions into the upper box and to increase the level of sequestration. The increase in the level of sequestration is due to the fact that the negative impact of adding carbon to the cycle via the lower box is damped by the slow exchange rate between the two boxes. The steady state values for the two taxes when $t \to \infty$ are

$$\psi_{ss} = \frac{D'_S}{\gamma + \rho} + \frac{\gamma}{\gamma + \rho}\pi_{ss}, \quad \pi_{ss} = \frac{\gamma\omega}{\rho + \gamma\omega}\psi_{ss} \tag{15}$$

or both equations solved for ψ_{ss} and π_{ss}

$$\psi_{ss} = \frac{(\rho + \gamma\omega)D'_S}{\rho(\gamma + \rho + \gamma\omega)}, \quad \pi_{ss} = \frac{(\gamma\omega)D'_S}{\rho(\gamma + \rho + \gamma\omega)}. \tag{16}$$

The first term of the steady state value for ψ_{ss} in (15) is equal to steady state values of models that include a constant rate of decay and therefore a proportional decay. In these models, the emission tax is equal to marginal damage, discounted by the interest rate and the duration of the carbon stock, whereas the latter is the constant decay rate. In our case, this decay rate is γ, which enters the movement equation like a constant decay rate if one expands the parenthesis in (1). Under the proportional decay assumption, the steady state would indicate a situation with constant marginal damage and a constant stock of carbon, whereby the amount of emissions would be equal to the amount of decay. In our case, the marginal damage can decrease during some time interval, but will be increasing in the long run as long as carbon is added to the cycle. Therefore, we retain the findings of Farzin and Tahvonen [4] that under the assumption of a choke or backstop price and nonrenewable elements of the atmospheric carbon stock, it is only optimal to extract until the discounted stream of persistent marginal damage is equal to the backstop price. In our nonrenewable resource two-box model, the constant rates do not express the proportional amount of carbon that vanish from the cycle, but the proportional amount of carbon that enters the other box. Consequently, a second term appears in the steady state value for ψ_{ss}. The second term indicates the influence of the sequestration tax on the emission tax. This term and the steady state value for π have the same structure. Both indicate the discounted fraction that either stock contributes to the other stock,

weighted by the tax corresponding to the other carbon stock. The combination of these two taxes describes the accumulation of carbon in the system, which is limited by the fraction of carbon present in the atmosphere. This can also be seen from (16). Given the purpose of the parameter values, γ and ω, ψ_{ss} is greater than π_{ss}. The difference between these two taxes, $\lambda = \psi - \pi$, is not just positive in the steady state but also throughout the whole planning period. The equation of motion for the tax difference

$$\dot{\lambda} = (\gamma + \gamma\omega + \rho)\lambda - D'(S), \tag{17}$$

indicates that the transversality condition $\lim_{t\to\infty} e^{-rt}\lambda \geq 0$ would be violated when λ becomes negative, because the marginal damage cannot become negative. The positive tax difference can also be seen from (10) and (11), because the only nonhomogeneous element in these two differential equations is the marginal damage in the equation of motion for the upper box. The influence of this element on the dynamics is transferred to the equation of motion for the lower box, but only damped, as ψ is multiplied by $\gamma\omega$ in(11). As result, not only the value of ψ but also the amplitude is greater than the value of π. Since the amount of extraction and sequestration varies by the levels of the two taxes, we investigate the possible paths of the two taxes.

Proposition 1. *The paths for the emission tax, ψ, the sequestration tax, π, and the tax difference, λ, are either monotonically increasing or U-shaped when it is optimal to take action at all.*

The proof can be found in Appendix Section 5.1, where we also show that when the path of π is U-shaped, the path of ψ has to be U-shaped as well, but when the path of ψ is U-shaped, π can be U-shaped or monotonically increasing. However, the ψ and λ always follow the same path. Therefore, extraction will either be monotonically decreasing or inversely U-shaped, and sequestration will either be monotonically increasing or U-shaped. The reverse effect on the two control variables indicates that we cannot assume an interior solution and therefore have to include the Kuhn-Tucker conditions in the analysis of the dynamics of the system.

3.3 Specific Results

Our qualitative analysis has indicated that the different movement tendencies for q and a give reason to carefully check the Kuhn-Tucker conditions. Applying the functional forms where the parameters

b, u_2, a_1, a_2, v_1, and s are positive,

$$\begin{aligned} U(q) &= bq - u_2 q^2, && (18)\\ A(a) &= a_1 a + a_2 a^2, && (19)\\ D(S) &= v_1 (sS - A_{preind})^2, && (20) \end{aligned}$$

we derive the necessary conditions from the current value Lagrangian

$$\begin{aligned} b + \theta_1 - 2u_2 q - \psi &= 0, && (21)\\ -a_1 - \theta_1 + \theta_2 - 2a_2 a + \psi - \pi &= 0, && (22)\\ -2v_1 s^2 S + 2v_1 s A_{preind} - \gamma\pi &= \dot{\psi} - \psi(\rho + \gamma), && (23)\\ -\gamma\omega\psi &= \dot{\pi} - \pi(\rho + \gamma\omega), && (24)\\ \theta_1 &\geq 0 \quad (\theta_1 = 0 \quad \text{if} \quad a - q < 0), && (25)\\ \theta_2 &\geq 0 \quad (\theta_2 = 0 \quad \text{if} \quad -a < 0), && (26) \end{aligned}$$

and obtain the canonical system:

$$\begin{pmatrix} \dot{\psi} \\ \dot{\pi} \\ \dot{S} \\ \dot{W} \end{pmatrix} = \begin{pmatrix} \rho+\gamma & -\gamma & -2s^2 v_1 & 0 \\ -\gamma\omega & \gamma\omega+\rho & 0 & 0 \\ -\frac{1}{2u_2} & 0 & -\gamma & \gamma\omega \\ 0 & 0 & \gamma & -\gamma\omega \end{pmatrix} \cdot \begin{pmatrix} \psi \\ \pi \\ S \\ W \end{pmatrix} + \begin{pmatrix} 2v_1 s A_{preind} \\ 0 \\ \frac{a2(b+\theta_1)+(a_1+\theta_1-\theta_2)u2}{2a_2 u_2} \\ -\frac{a_1}{2a_2} - \frac{\theta_1}{2a_2} + \frac{\theta_2}{2_a 2} \end{pmatrix}. \quad (27)$$

The steady state values for the canonical system when $t \to \infty$ are

$$\begin{aligned} \psi_{ss} &= b + \theta_1, && (28)\\ \pi_{ss} &= \frac{(b+\theta_1)\gamma\omega}{h_2}, && (29)\\ S_{ss} &= \frac{2sA_{preind}v_1 h_1 + b\rho h_2}{2s^2 v_1 h_1} + \frac{\theta_1 \rho h_1}{2s^2 v_1 h_2}, && (30)\\ W_{ss} &= \frac{2sA_{preind}v_1 h_1 + b\rho h_2}{2s^2 v_1 \omega h_1} + \frac{\theta_1 \rho h_1}{2s^2 v_1 \omega h_2} + \frac{b\rho - a_1 h_2}{2a_2\gamma\omega h_2} - \frac{\theta_1}{2a_2 h_2} + \frac{\theta_2}{2a_2\gamma\omega}, && (31)\\ & \text{with} \quad h_1 = \gamma + \rho + \gamma\omega, \quad \text{and} \quad h_2 = \rho + \gamma\omega. \end{aligned}$$

For the Kuhn-Tucker conditions, we have to consider four different cases:

Case 1: Both constraints are inactive, $q - a \geq 0$ and $a \geq 0$. This case describes positive extraction and sequestration whereby not the total amount of fossil fuels extracted is sequestered. We obtain $\theta_1 = \theta_2 = 0$.

Case 2: Constraint one is inactive, constraint two is active, $q-a \geq 0$ and $a = 0$. This case describes positive extraction and no sequestration. We obtain $\theta_2 = \pi + a_1 - \psi$.

Case 3: Constraint one is active, constraint two is not, $q - a = 0$ and $a \geq 0$. This case describes positive extraction and sequestration whereby the total amount of fossil fuels extracted is sequestered. We obtain $\theta_1 = 2u_2 q + \psi - b$ and $\theta_1 = -a_1 - 2a_2 a + \psi - \pi$, and therefore $q = a = \frac{b-a_1-\pi}{2(u_2+a_2)}$ and $\theta_1 = \psi - \pi\frac{u_2}{a_2+u_2} - \frac{a_2 b + a_1 u_2}{a_2+u_2}$.

Case 4: Both constraints are active, $q-a = 0$ and $a = 0$. This case describes no activity at all, zero extraction and zero sequestration. We obtain the values $\theta_1 = b - \psi$ and $\theta_2 = b - a_1 - \pi$.

Four possible steady state situations emerge from the four different cases . Regarding the nonrenewable feature of the two-box model, in each of the 4 cases the FOCs, (21) and (22), must yield $q = a = 0$ and the exchange term in the equations of motion, (1) and (2), must satisfy $(S - \omega W) = 0$ in an admissible steady state solution. In a first step we investigate each case and check under which conditions the steady state is admissible.

1. The steady state values for the first case, $\theta_1 = \theta_2 = 0$, are admissible and unique if $a_1 = b\frac{\rho}{\rho+\gamma\omega}$. FOC (21) implies $q = 0$ for $\psi_{ss} = b$ and FOC (22) implies $a = 0$ if

$$b - b\frac{\gamma\omega}{\rho+\gamma\omega} - a_1 = 0 \quad \Rightarrow \quad a_1 = b\frac{\rho}{\rho+\gamma\omega}. \tag{32}$$

   The condition $(S - \omega W) = 0$ is satisfied if the third term in the steady state value for W_{ss} is zero. The second, fourth, and fifth terms in the steady state value for W_{ss} are zero for the first case, and the first terms in the steady state values for S_{ss} and W_{ss} differ only by the parameter ω in the denominator of W_{ss}. The third term is zero if

$$\frac{b\rho - a_1(\rho+\gamma\omega)}{2a_2\gamma\omega(\rho+\gamma\omega)} = 0 \quad \Rightarrow \quad a_1 = b\frac{\rho}{\rho+\gamma\omega}. \tag{33}$$

2. The steady state values for the second case, $\theta_1 = 0$ and $\theta_2 > 0$, are admissible and unique, if $a_1 > b\frac{\rho}{\rho+\gamma\omega}$. FOC (21) implies $q = 0$ for $\psi_{ss} = b$ and FOC (22) implies $a = 0$ if

$$b - b\frac{\gamma\omega}{\rho+\gamma\omega} - a_1 + \theta_2 = 0 \quad \Rightarrow \quad a_1 = b\frac{\rho}{\rho+\gamma\omega} + \theta_2. \tag{34}$$

   The condition $(S - \omega W) = 0$ is satisfied if the sum of the third and fifth term in the steady state value for W_{ss} is zero. The second and fourth terms in the steady state value for W_{ss} are

zero for the second case. The sum of the third and fifth term is zero if

$$\frac{b\rho - a_1(\rho+\gamma\omega)}{2a_2\gamma\omega(\rho+\gamma\omega)} + \frac{\theta_2}{2a_2\gamma\omega} = 0 \quad \Rightarrow \quad a_1 = b\frac{\rho}{\rho+\gamma\omega} + \theta_2. \tag{35}$$

3. The steady state values for the third case, $\theta_1 > 0$ and $\theta_2 = 0$, are admissible, if $a_1 < b\frac{\rho}{\rho+\gamma\omega}$. For a given level of a_1 that satisfies the last condition, the steady state is unique. FOC (21) implies $q = 0$ for $\psi_{ss} = b + \theta_1$ and FOC (22) implies $a = 0$ if

$$b + \theta_1 - (b+\theta_1)\frac{\gamma\omega}{\rho+\gamma\omega} - a_1 - \theta_1 = 0 \quad \Rightarrow \quad a_1 = b\frac{\rho}{\rho+\gamma\omega} - \theta_1\frac{\gamma\omega}{\rho+\gamma\omega}. \tag{36}$$

The condition $(S - \omega W) = 0$ is satisfied if the sum of the third and fourth term in the steady state value for W_{ss} is zero. The fifth term in the steady state value for W_{ss} is zero in the third case and the second terms in the steady state values for S_{ss} and W_{ss} differ only by the parameter ω in the denominator of W_{ss}. The sum of the third and fourth term is zero if

$$\frac{b\rho - a_1(\rho+\gamma\omega)}{2a_2\gamma\omega(\rho+\gamma\omega)} - \frac{\theta_1}{2a_2(\rho+\gamma\omega)} = 0 \quad \Rightarrow \quad a_1 = b\frac{\rho}{\rho+\gamma\omega} - \theta_1\frac{\gamma\omega}{\rho+\gamma\omega}. \tag{37}$$

4. The steady state values for the fourth case, $\theta_1 > 0$ and $\theta_2 > 0$, are admissible, if $a_1 \lessgtr b\frac{\rho}{\rho+\gamma\omega}$. The admissibility of the steady state does not depend on the level of a_1. The steady state is not unique for a given level of a_1. FOC (21) implies $q = 0$ for $\psi_{ss} = b + \theta_1$ and FOC (22) implies $a = 0$ if

$$b + \theta_1 - (b+\theta_1)\frac{\gamma\omega}{\rho+\gamma\omega} - a_1 - \theta_1 + \theta_2 = 0 \quad \Rightarrow \quad a_1 = b\frac{\rho}{\rho+\gamma\omega} - \theta_1\frac{\gamma\omega}{\rho+\gamma\omega} + \theta_2. \tag{38}$$

The condition $(S - \omega W) = 0$ is satisfied, if the sum of the third, fourth, and fifth term is zero. The sum is zero if

$$\frac{b\rho - a_1(\rho+\gamma\omega)}{2a_2\gamma\omega(\rho+\gamma\omega)} - \frac{\theta_1}{2a_2(\rho+\gamma\omega)} + \frac{\theta_2}{2a_2\gamma\omega} = 0 \quad \Rightarrow \quad a_1 = b\frac{\rho}{\rho+\gamma\omega} - \theta_1\frac{\gamma\omega}{\rho+\gamma\omega} + \theta_2. \tag{39}$$

The admissible steady state values do not differ for the first and the second case. This fact can be seen by noticing that θ_2 only enters into the steady state value expression of W_{ss}. If the steady state for the third case is admissible, the Kuhn-Tucker multiplier θ_1 enters into the steady state value expression for ψ_{ss}, π_{ss}, S_{ss}, and W_{ss} with a positive sign. As a result, the steady state values are greater for the third case than for the first and second case. We solve the critical parameter combination for a_1 to indicate the admissability of the steady states. If a_1 is equal or greater than

$b\frac{\rho}{\rho+\gamma\omega}$ the smaller steady state is admissible, the greater one is not. If a_1 is less than this level, the smaller steady state is not admissible, the greater steady state is. The smaller steady state does not vary in size due to variations in a_1; the greater steady state increases its size when a_1 decreases. Due to its impact on the size of the steady state values, we denote the critical parameter combination for a_1 as the critical level:

$$a_{crit} = b\frac{\rho}{\rho + \gamma\omega}. \tag{40}$$

The admissible steady state values for the fourth case are greater than the corresponding steady state values for a given level of a_1 in case 1, 2, or 3. The steady state values for the fourth case have to be greater than the ones in the first and second case, because in the first and second cases θ_1 does not enter into the steady state value expressions. The steady state values for the fourth case have to be greater than for the third case, because it can be seen from conditions (36) and (38) that θ_1 has to be greater in the fourth case than in the third case for a given level of a_1. The varying size of the steady state values matters especially for the two state variables, S and W, because it implies various carbon stabilization levels in the upper and lower boxes.

Proposition 2. *If at least one Kuhn-Tucker condition is inactive in the steady state, the steady state values are uniquely determined by the parameter values. The unique steady state is characterized either by* $a_1 \geq a_{crit}$, $\theta_1 = 0$, *and* $\theta_2 \geq 0$ *or by* $a_1 < a_{crit}$, $\theta_1 > 0$, *and* $\theta_2 = 0$. *The former combination provides smaller steady state values than the latter.*

In the next step we analyze the dynamics toward the steady state. Depending on which Kuhn-Tucker condition is active, we can divide the control space into four different regimes:

Regime 1: *Moderate Sequestration:* $q > a > 0$

Regime 2: *No sequestration:* $q > 0$ and $a = 0$

Regime 3: *Complete Sequestration:* $q = a > 0$

Regime 4: *No activity:* $q = a = 0$

We consider each regime as a singular dynamic system and check if it converges straight to a unique steady state, or, if not, to which other regime it switches. The canonical systems and the corresponding steady state values for each regime can be found in Appendix Section 5.2. The dynamics can be distinguished by the possible tax paths.

Scenario 1. *The initial values for the state variables,* S *and* W*, are low and the paths of the two taxes,* ψ *and* π *are monotonically increasing.*

Scenario 2. *The initial value is high for the state variable S and low for the state variable W. The paths of the two taxes, ψ and π, are U-shaped. The sum of the initial values is smaller than the sum of the specific steady state values, $S_{ss} + W_{ss}$, which correspond to the specific level of a_1.*

We investigate the dynamic system for both scenarios in particular. First we consider Scenario 1, which implies that the path of the tax difference, λ, is monotonically increasing as well. The taxes and their difference increase monotonically toward their steady state values. As a consequence the initial levels of the taxes and their difference have to be smaller than their steady state values and we can rule out Regime 4 as an initial regime under Scenario 1. Regimes 1, 2, and 3 remain possible regimes to describe the dynamics towards the steady state. However, in the situation where a_1 is greater than or equal to its critical level, only Regime 2 can occur. The condition $\theta_2 = \pi_{ss} - \psi_{ss} - a_1 \geq 0$ is still fulfilled in the steady state for $a_1 \geq a_{crit}$. For π to be monotonically increasing towards its steady state value, the tax difference has to reach its maximum in the steady state. Consequently, the dynamic system is described completely by Regime 2 and converges to the unique steady state that is characterized by the smaller steady state values. On the path towards the steady state, the amount of extraction monotonically decreases towards zero, the amount of sequestration is constantly zero, and the stocks of carbon in the upper and in the lower box monotonically increase towards their steady state values.

When a_1 is below its critical level, θ_2 has to become negative when the dynamic system moves towards the steady state. When θ_2 becomes negative, sequestration becomes positive, the dynamic system switches towards Regime 1, with both extraction and sequestration being positive, but the latter being smaller than the former. However, as the emission tax; ψ, and the tax difference, λ, continue to monotonically increase, the amount of extraction decreases and the amount of sequestration increases. As a consequence, a second switching point emerges, when the path of extraction and sequestration intersect. After this point in time, the first Kuhn-Tucker condition becomes binding and the dynamic system switches towards Regime 3, which implies that the amount of extraction and sequestration are equal. The Kuhn-Tucker multiplier $\theta_1 = \psi - \pi\frac{u_2}{a_2+u_2} - \frac{a_2 b + a_1 u_2}{a_2+u_2}$ remains positive after the switching point because the tax difference is monotonically increasing towards the steady state. However, the amount of extraction and sequestration are solely determined by the level of π in Regime 3. As a result, both amounts are monotonically decreasing. The dynamic system converges to the unique steady state which is characterized by the greater steady state values due to the fact $a_1 < a_{crit}$. On the path to the steady state, the amount of extraction monotonically decreases towards zero. The amount of sequestration is initially constant zero until the first switching point. Then it increases monotonically until the second switching point. Thereafter, it follows the same path as extraction and decreases monotonically towards zero. The stock of carbon in the

upper and lower box increase monotonically towards their steady state values, whereby the amount of carbon in the upper box increases after the second switching point only by the natural transfer rate. The more a_1 is below its critical level, the earlier the dynamic system switches from Regime 2 to Regime 1. As both taxes and their difference start at positive initial levels, there exists a level of a_1 for which the dynamic system directly starts in Regime 1. In this situation, the dynamics follow the same pattern as in the case of initial Regime 2 after the first switching point. When it holds true that $\psi_0(\frac{u_2+a_2}{u_2} - \frac{\gamma\omega}{\gamma\omega+\rho} - a_1) - b\frac{a_2}{u_2} - a_1 > 0$ is fulfilled, the dynamic system even starts directly in Regime 3. For this situation to happen, a_1 and a_2 have to be rather small which implies that sequestration costs are very low. The dynamics then follow the same pattern as in the case of initial Regime 2 after the second switching point.

Proposition 3. *Given Scenario 1: When a_1 is greater than or equal to its critical level, the dynamic system starts in Regime 2 and remains there on the complete path toward the steady state. When a_1 is smaller than its critical level, the succession of regimes is either 2, 1, 3 or 1, 3 or only 3, however, the dynamics towards the steady state are uniquely determined by Regime 3.*

In Appendix Section 5.2, we show that the steady state values of Regime 2 are smaller than the ones of Regime 3 when a_1 is below its critical level. This result is line with Proposition 2. In Figure 1, we show the numerical solution for Scenario 1 and the two situations $a_1 = a_{crit}$ and $a_1 < a_{crit}$.[10] In the left window, we see that the optimal path for the situation $a_1 = a_{crit}$. In the right window, we see the optimal path for the situation $a_1 < a_{crit}$. For our parameter values, the succession of regimes is 2, 1, and 3. However, the first switching point emerged already after 4 time units, so we do not show it in the graphic. That implies that we would have started directly in Regime 1 for slightly lower sequestration costs. We did not find a parameter combination that provided initial Regime 3 for Scenario 1. The analytical determination whether Regime 3 can occur as initial regime requires the inclusion of the eigenvectors in their analytical form. Unfortunately, the analytical representation of the eigenvectors is too complex to allow a comprehensible investigation. Therefore, we make do with the proposition that Regime 3 might occur as initial regime under Scenario 1, however, the necessary parameter combination might describe a rather bizarre situation.

We turn now to the case, where the paths of both taxes are U-shaped. Scenario 2 implies that the path of the tax difference, λ, is U-shaped as well. However, also for the U-shaped case, the paths of the taxes approach their steady state values from below. As a consequence, the results under Scenario 1 apply again for the movement of the dynamic system into the steady state. Depending

[10] We formulated this nonlinear constrained optimization problem in AMPL and solved it with the Knitro algorithm. The parameter values are $b = 60$, $\gamma = 1/200$, $\omega = 1/10$, $\rho = 2/100$, $a_2 = 2$, $u_2 = 1$, $v_1 = 0.0875$, $s = 3/10$, and $A_{preind} = 600$. These parameter values yield $a_{crit} = 58.5366$. For the second situation, $a_1 < a_{crit}$, the parameter value for a_1 is 45. The initial value for W_0 is 20000 Gt C in both situations.

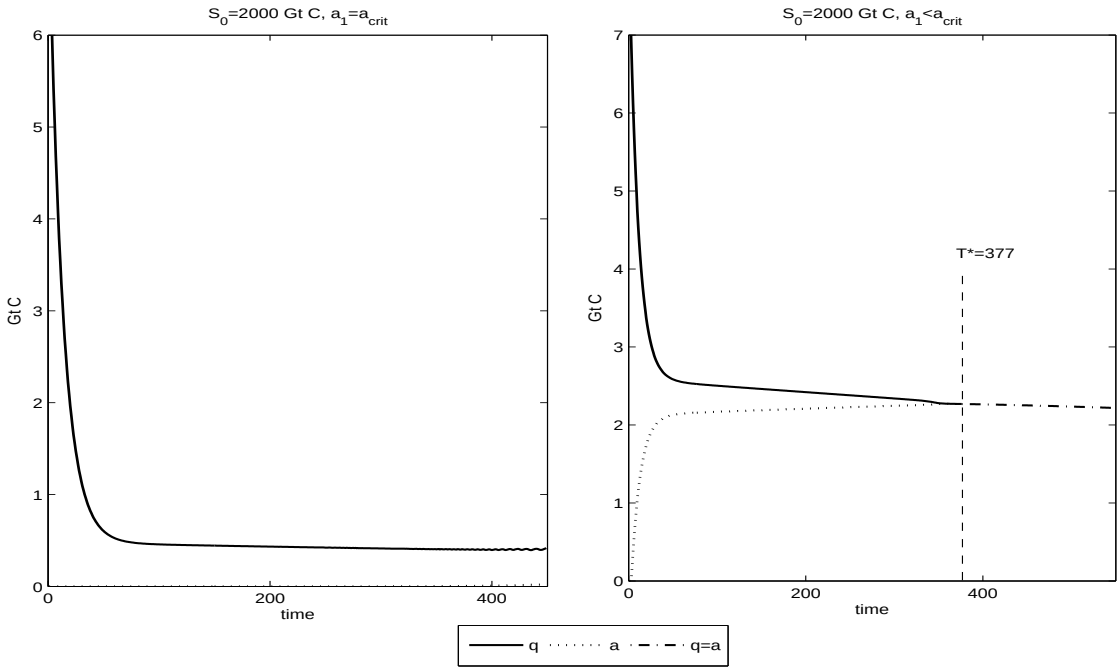

Figure 1: Numerical solution for q and a for Scenario 1

on the level of a_1, the final regime leading to the steady state is described either by Regime 2 or Regime 3, no matter which regimes previously occurred. The occurrence of the previous regimes can be distinguished by the levels of S_0 and the level of a_1. We describe the possible dynamics by considering each of the four regimes as an initial regime. Again, we investigate first the situation where a_1 is greater than or equal to its critical level whereby the final movement into the steady state is described by Regime 2.

1. Initial Regime 1 implies initial values for the taxes that lead to $q > a > 0$. For this situation to occur, we have to observe $\psi_0 < \psi_{ss}$, but $\lambda_0 > \lambda_{ss}$. The second condition implies that $S_0 > S_{ss}$ and $\pi_0 << \pi_{ss}$, otherwise the tax difference could not be U-shaped. As both taxes and their difference are first decreasing, the amount of extraction increases and the amount of sequestration decreases. Therefore, a point in time emerges when $\lambda_t = \lambda_{ss}$ and the dynamic system switches to Regime 2, within which it remains on the path towards the steady state. The path of extraction is inversely U-shaped, the path of sequestration is monotonically decreasing towards zero at the switching point and is constantly zero thereafter.

2. Initial regime 2 implies initial values for the taxes that lead to $q > 0$ and $a = 0$. For this situation to occur, we have to observe $\psi_0 < \psi_{ss}$ and $\lambda_0 < \lambda_{ss}$. The U-shaped path for the tax difference implies that λ is below its steady state value the whole time. Therefore, the dynamic system remains in Regime 2. The path of extraction is inversely U-shaped, and the

path of sequestration is constantly zero.

3. Initial Regime 3 implies initial values for the taxes that lead to $q = a > 0$. For this situation to occur, we have to observe $\pi_0 < \pi_{ss}$ and $\lambda_0 > \lambda_{ss}$. The second condition implies $S_0 > S_{ss}$. The decreasing paths of the taxes and their difference implies that a point in time emerges, when θ_1 becomes negative and the dynamic system switches to Regime 1. This implies that $\psi_t < \psi_{ss}$ and $\pi_t < \pi_{ss}$ but still $\lambda_t > \lambda_{ss}$. As the taxes continue to decrease, another point in time emerges when $\lambda_t = \lambda_{ss}$ and the dynamic system switches to Regime 2 within which it remains on the path towards the steady state. In the initial regime the amounts of extraction and sequestration follow the same path, which is monotonically increasing. After the first switching point the path of extraction continues to increase, whereas the path of sequestration decreases monotonically towards zero. After the second switching point, the path of extraction is inversely U-shaped and the path of sequestration is constantly zero.

4. Initial Regime 4 implies initial values for the taxes that lead to $q = a = 0$. For this situation to occur we must observe $\psi_0 > \psi_{ss}$ and $\pi_0 > \pi_{ss}$. The upper and lower boxes adjust solely due to natural forces until the dynamic system switches from Regime 4 to Regime 3 which implies $\pi_t < \pi_{ss}$. Thereafter, the behavior of the dynamic system is equal to the previous case, where the initial regime is Regime 3.

Now, we consider the situation where a_1 is smaller than its critical level whereby the final movement into the steady state is described by Regime 3.

1. Initial Regime 1 implies initial values for the taxes that lead to $q > a > 0$. For this situation to occur, we have to observe $\psi_0 < \psi_{ss}$, $\pi_0 < \pi_{ss}$, and $\lambda_0 < \lambda_{ss}$. The U-shaped paths of the taxes and their difference allow two different successions of regimes. When the minimum of the tax difference is smaller than a_1, the dynamic system switches towards Regime 2 on the decreasing part of the path and switches back to Regime 1 after the minimum of λ has occurred and the taxes are increasing again. When the minimum of the tax difference is greater than a_1, the dynamic system remains within Regime 1, on the path through the minimum. However, in both cases, there emerges a point in time on the increasing part of the tax paths when the dynamic system switches to Regime 3 and remains there on the path towards the steady state. In both successions, the path of extraction is inversely U-shaped. When it holds true that $\lambda_{min} < a_1$, the path of sequestration is monotonically decreasing towards zero, is constantly zero between the first and second switching point, and is monotonically increasing until the third switching point. Thereafter, it follows the same path as extraction and decreases monotonically towards zero. When it holds true that $\lambda_{min} \geq a_1$, the path of sequestration is

U-shaped until the only switching point, thereafter, it follows the same path as extraction and decreases monotonically towards zero.

2. Initial Regime 2 implies initial values for the taxes that lead to $q > 0$ and $a = 0$. For this situation to occur, we have to observe $\psi_0 < \psi_{ss}$, $\pi_0 < \pi_{ss}$, $\lambda_0 < \lambda_{ss}$ and additionally $\lambda_0 < a_1$ with $\theta_2 > 0$. In this case, the U-shaped paths of the taxes and their difference allow only one succession of regimes. The dynamic system remains in Regime 2 until it holds true that $\lambda_t > a_1$, which can only occur when the dynamic system is on the increasing part of the paths again. At that point in time, it switches to Regime 1. As the taxes continue to increase, another point in time emerges when the dynamic system switches to Regime 3 and remains there on the path towards the steady state. The path of extraction is inversely U-shaped, the path of sequestration is constantly zero until the first switching point, is monotonically increasing until the second switching point, and is then monotonically decreasing on the same path as extraction towards zero.

3. Initial Regime 3 implies initial values for the taxes that lead to $q = a > 0$. For this situation to occur, we have to observe $\psi_0 \lessgtr \psi_{ss}$, $\pi_0 < \pi_{ss}$, $\lambda_0 \lessgtr \lambda_{ss}$ and additionally $\lambda_0 > a_1$ with $\theta_1 > 0$. The U-shaped paths of the taxes and their difference allow three different successions of regimes. When the minimum of the tax difference is smaller than a_1, the dynamic system switches first to Regime 1 and thereafter to Regime 2 on the decreasing part of the taxes and switches back to Regime 1 after the minimum of λ has occurred and the taxes are increasing again. When the minimum of the tax difference is greater than a_1 but at that point in time θ_1 is negative, the dynamic system switches to Regime 1 and remains there on the path through the minimum of λ. However, in both cases, there emerges a point in time on the increasing part of the taxes when the dynamic system switches to Regime 3 and remains there on the path towards the steady state. When the minimum of the tax difference is greater than a_1 and at that point in time θ_1 is positive, the dynamic system is in Regime 3 the whole time. In all three successions, the path of extraction is inversely U-shaped. For the first succession, the path of sequestration is first monotonically increasing until the first switching point, is monotonically decreasing toward zero until the second switching point, is constantly zero until the third switching point, is monotonically increasing until the fourth switching point and is then monotonically decreasing on the same path as extraction towards zero. For the second succession, there are only two switching points and the path of sequestration is similar to the first succession without the part where it is constantly zero. Between the two remaining switching points the path of sequestration is U-shaped. For the third succession, the path of

sequestration is inversely U-shaped on the same path as extraction.

4. Initial Regime 4 implies initial values for the taxes that lead to $q = a = 0$. For this situation to occur, we have to observe $\psi_0 > \psi_{ss}$, $\pi_0 > \pi_{ss}$, $\lambda_0 > \lambda_{ss}$ which implies $S_0 > S_{ss}$. The U-shaped paths of the taxes and their difference allow three different successions of regimes that are the same as in the previous case with initial Regime 3. The upper and lower boxes adjust solely due to natural forces until the dynamic system switches from Regime 4 to Regime 3 which implies $\pi_t < \pi_{ss}$. The possible paths of extraction and sequestration are the same as for initial Regime 3 except for the beginning, when both paths are constantly zero until the first switching point.

In both situations, $a_1 \geq a_{crit}$ and $a_1 < a_{crit}$, the path of S is U-shaped and the path of W is monotonically increasing. As already mentioned, the succession of the various regimes depends on the combination of various levels of S_0 and various levels of a_1. However, for a given level of a_1, we observe initial regimes in the order regime 2, regime 1, regime 3 and regime 4 for increasing levels of S_0. Especially initial regime 3 and 4 imply high initial levels for S. The description of the possible dynamics under Scenario 2 revealed that sequestration may also be used from the beginning when the initial conditions constitute a situation where the carbon cycle already differs substantially from the equilibrium distribution of carbon between the upper and lower boxes.

Proposition 4. *Given Scenario 2: All 4 regimes can occur as possible inital regimes. The succession of the various regimes is determined by the combination of various initial levels of S and various levels of a_1. The final regime is again uniquely determined by the level of a_1, which is either Regime 2 for $a_1 \geq a_{crit}$ or Regime 3 for $a_1 < a_{crit}$. In contrast to Assumption 1, the amount of sequestration may be positive for some time even when $a_1 \geq a_{crit}$.*

The description of the various successions for the 4 initial regimes includes all possible dynamics. However, some of the successions may only occur for some very special combinations of the initial levels of S and the parameter values, especially the level of a_1. As already mentioned, the complete analytical determination of the various dynamics would require the inclusion of the eigenvectors in their analytical form. However, the validity of Proposition 4 is not restricted. In Figure 2 we show the numerical solution for Scenario 2, various initial levels of S_0 above the preindustrial level, and the two situations $a_1 = a_{crit}$ and $a_1 < a_{crit}$.[11] In the left column the paths depict the solutions to the situation $a_1 = a_{crit}$, in the right column the paths depict the solutions to the situation $a_1 < a_{crit}$. In the left column, we have two different initial levels, the lower left window shows an enlargement

[11] We formulated this nonlinear constrained optimization problem in AMPL and solved it with the Knitro algorithm. The parameter values are the same as for figure 1. The initial level of W_0 is 20000 Gt C in each window.

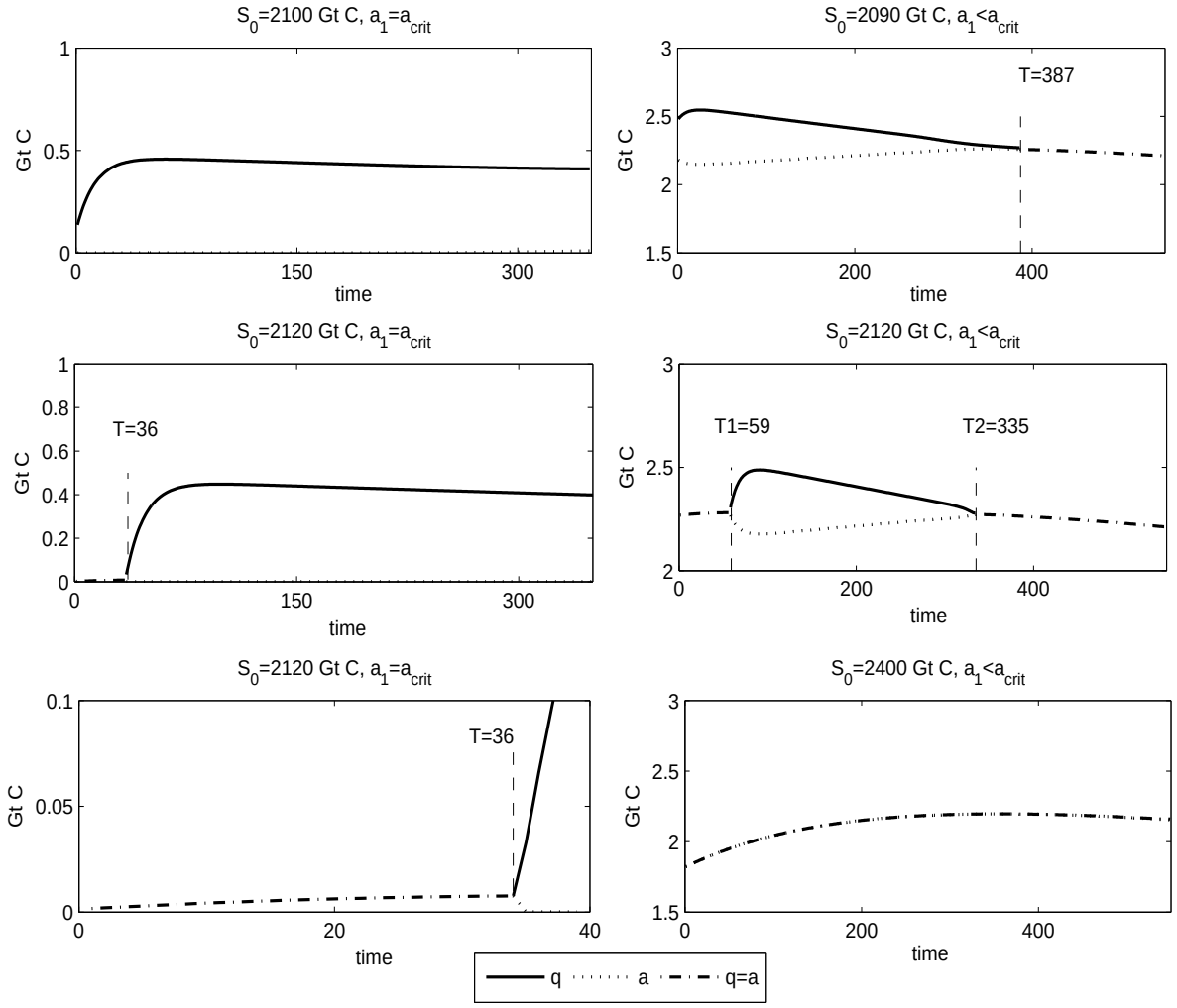

Figure 2: Numerical solution for q and a for Scenario 2

of the first part of the middle left window. In the right column, we have three different initial levels. The left column shows the optimal path for initial Regimes 2 and 3. The enlarged lower left window highlights the period of complete sequestration even for the situation $a_1 = a_{crit}$. We were not able to obtain a solution with initial Regime 1 for the given parameter values in the situation $a_1 = a_{crit}$. The right column shows the optimal paths for initial Regime 1 and 3. We were not able to obtain a solution with initial Regime 2 for the given parameter values in the situation $a_1 < a_{crit}$.

The investigation of the dynamics under Scenario 1 and 2 reveals that the dynamic system never switches to Regime 4. As a consequence, the dynamics towards the steady state are only determined by Regime 4 when the dynamic system is completely described by Regime 4. Under Scenario 2, Regime 4 appears as an initial regime when the initial level of S is greater than its steady state value associated with the specific level of a_1. In Scenario 2, however, we restrict the sum of the

initial values so that they are lower than the sum of the specific steady state values. As a result, the natural forces in Regime 4 cause the upper and lower boxes to adjust until it is optimal to be active again. Without this restriction, initial values can emerge for which the dynamic system remains in Regime 4 the whole time. The dynamics are completely determined by the adjustment of the two boxes by the natural forces. The resulting steady state values for Regime 4 depend therefore solely on the initial levels:

$$S_{ssr4} = \frac{\omega(S_0 + W_0)}{1+\omega}, \quad W_{ssr4} = \frac{S_0 + W_0}{1+\omega}. \tag{41}$$

The steady state values, S_{ssr4} and W_{ssr4}, apply to the fourth case in the steady state analysis, where both Kuhn-Tucker multipliers are positive. The values of θ_1 and θ_2 have to be chosen so that the general steady state value expressions (30) and (31) match the specific steady state values (41) and so that FOCs (21) and (22) are fulfilled. We already showed that steady state values for the case where $\theta_1 > 0$ and $\theta_2 > 0$ are greater than the corresponding steady state values for the specific level of a_1. This result is confirmed because it is the preliminary condition for the initial values for this case to occur. We can now extend Proposition 2:

Proposition 5. *When both Kuhn-Tucker conditions are active in the steady state, the steady state values are uniquely determined by the initial levels, S_0 and W_0. For this case, the dynamic system is solely described by Regime 4.*

In Appendix Section 5.3, we show the necessary parameter restriction so that Regime 2 and Regime 3 obey saddle path properties and that regime 4 obeys saddle path properties without parameter restrictions. Given the initial values for S and W at the initial or switching points, we can choose appropriate taxes so that the dynamic system converges to the steady state.

We complete our analysis by investigating the critical level, a_{crit}, which we use to determine the characteristics of the steady state and the dynamics towards it. If we choose another description of the sequestration cost function without a linear term, we can conclude that sequestration will always be utilized when it is optimal to take action at all. However, in our description of the sequestration cost function, the level of a_1 not only determines whether sequestration is just a temporary or the long-run option but also the extent to which sequestration is utilized. The levels of the steady state values increase when a_1 decreases given that $a_1 < a_{crit}$ is satisfied. The greater the distance between a_{crit} and a_1 for $a_{crit} > a_1$, the earlier sequestration is utilized and the earlier the complete amount of extracted carbon is sequestered. Consequently, an increase in a_{crit} increases the effectiveness of sequestration for a given level of a_1. The effectiveness of sequestration in this two-box model depends crucially on generating utility by using fossil fuels while delaying the resulting damage

due to increased levels of carbon in the atmosphere into the future. As result, the effectiveness of sequestration depends on the time preferences and the adjustment times of the two boxes. The critical level, a_{crit}, is determined by the discount factor and the adjustment parameters of the two-box model. When the discount factor decreases, the critical level decreases as well. As a result, the effectiveness of sequestration decreases because, with a lower discount factor, delaying damages pays off less. When γ and ω decrease, the critical level increases. As a result, the effectiveness of sequestration increases because, with lower adjustment factors, the adjustment time of the two boxes decreases. A smaller value for γ implies a slower mixing of the two boxes. A smaller value for ω implies a greater lower box, which in turn implies that the lower box can contain greater amounts of carbon. The adjustment factors, γ and ω, can be estimated so that no variation in the prohibitive level by them should arise. However, while approximating the carbon cycle with a two-box model, varying the mixing speed and in the size of the lower box accounts for various assumptions about the amount of carbon in the lower box that is active when it is in the equilibration process with the upper box. In the context of our model, variations in the amount of carbon active in the lower box can be used to approximate various injection depths for carbon sequestration. A deeper injection depth goes along with a greater lower box and a slower adjustment process. Therefore, the effectiveness of sequestration depends on the injection depth. Nevertheless, this conclusion depends on the fact that the two adjustment factors may vary. In general, these two factors describe the effectiveness of sequestration due to the inertia of the carbon cycle. Both factors are comparatively low in relation to common discount factors, which implies that the critical level is close to the backstop price.

4 Conclusions

In this paper, we investigate optimal anthropogenic intervention into the global carbon cycle. We applied a simple two-box model to include the atmospheric and the oceanic carbon reservoirs. The two-box model allows us to analyze aspects of the global carbon cycle in a more appropriate way than a simple proportional decay model. Therefore, the resulting steady states in our model differ clearly from those resulting in proportional decay models. In our model fossil fuel extraction is halted because of dangerous level of carbon in the atmosphere and not because fossil reserve run out. This result is based on the nonrenewable features of the two-box model as well as on the assumption that there is a choke price in our utility function for fossil fuel extraction. Additionally, we included the option to sequester carbon by capturing CO_2 and injecting it into the deep ocean. The sequestration option does not constitute a backstop technology, as carbon is not removed from the two-box model. The amount of extraction is determined by an emission tax and the amount of

sequestration is determined by the difference between the emission tax and an sequestration tax. We show that the taxes are either monotonically increasing for low initial levels of the upper box or U-shaped for high initial levels of the upper box. After introducing quadratic-linear functional forms, we used the linear term in the sequestration cost function to express the parameter combination that distinguishes the steady states and the dynamics. We derived a critical level for this linear term that indicates whether the movement towards the steady state is described either by sole extraction and zero sequestration or by complete sequestration of the extracted amount. The steady state values for the former case are smaller than for the latter case, implying that a final period of complete sequestration leads to higher stabilization levels in the atmosphere and the ocean. The dynamics before the movement towards the steady state are described either by sole extraction, extraction and sequestration, complete sequestration, or even a period of inaction depending on the initial levels of carbon in the upper box. Even with high sequestration costs, sequestration might be used as temporary option, whereby with low sequestration costs, it constitutes the long-run option allowing extended use of fossil fuels. The effectiveness of sequestration depends on the effect of delaying the atmospheric carbon stock damage associated with fossil energy use. Consequently, the critical level for the linear term in the sequestration cost function depends on the discount factor and the adjustment parameters of the two-box model. A lower discount factor and a faster adjustment of the two the boxes reduces the effectiveness of sequestration. We interpreted the variation in the adjustment parameters of the two boxes as constituting a measure for various injection depths for carbon sequestration.

Our two-box model is a strong simplification of the global carbon cycle. The exchange between the two boxes is linear and therefore excludes feedback mechanisms in the global carbon cycle. This simplification is justified to some extent for moderate carbon disturbances like a doubling of the preindustrial level in the atmospheric reservoir. In order to obtain a better description of the global carbon cycle, more boxes would have to be included, the different carbon pumps would have to be modeled separately, and feedback mechanisms would have to be incorporated. Nevertheless, the purpose of our model is not to predict various carbon stabilization levels for the atmosphere and the ocean, but to incorporate in a stylized way important aspects of the global carbon cycle. Additionally, we allowed carbon to be released to another reservoir than the atmosphere, i.e., we allowed ocean sequestration. Without sequestration, the limiting factor, besides the accumulation of carbon in the atmosphere, is the inertia of the system to transport carbon from the atmosphere to the other reservoirs. With sequestration, it would be possible to show that carbon distribution between the atmosphere and the ocean deviates less from the equilibrium distribution, which is what we do in a following paper. Even with high sequestration costs, ocean sequestration can still be used

as a temporary option to adjust large initial disequilibrium carbon distributions. Further research might investigate the carbon cycle adjusting aspects of sequestration for various stabilization goals under the explicit inclusion of a backstop technology.

References

[1] Canadell, J., Quere, C. L., Raupach, M., Field, C., Buitehuis, E., Ciais, P., Conway, T., Gillett, N., Houghton, R., and Marland, G., Contributions to accelerating atmospheric CO_2 growth from economic activity, carbon intensity, and efficiency of natural sinks. , PNAS (2007) 1–5.

[2] Chiang, A. C., Elements of Dynamic Optimization (first ed.), McGraw-Hill, Inc., 1992.

[3] Dockner, E.,Local stability analysis in optimal control problems with two state variables, in G. Feichtinger (Ed.), Optimal Control Theory and Economic Analysis 2, Elsevier Science Publishers B.V., New York, 1985, pp. 89–104.

[4] Farzin, Y., and Tahvonen, O., Global Carbon Cycle and the Optimal Time Path of a Carbon Tax, Oxf. Econom. Papers 48 (1996) 515–536.

[5] Forster, B.A., Optimal pollution control with a nonconstant exponential rate of decay, J. Environ. Econom. Management 2 (1975) 1–6.

[6] Herzog, H., Caldeira, K., and Reilly, J., An issue of permancence: Assessing the effectiveness of temporary carbon storage, Climatic Change 59 (2003) 293–310.

[7] IPCC, Special report: Carbon dioxide capture and storage, Intergovernmental Panel on Climate Change, Cambridge UK, 2005.

[8] Körtzinger, A., and Wallace, D., Der globale Kohlenstoffkreislauf und seine anthropogene Störung - eine Betrachtung aus mariner Perspektive, promet 28, 1/2 (2002) 64–70.

[9] Maier-Raimer, E., and Hasselmann, K., Transport and storage of CO_2 in the ocean - an inorganic ocean-circulation carbon cycle model, Climate Dynamics 2 (1987) 63–90.

[10] Najjar, R., Marine biogeochemistry, in K. E. Trenberth (Ed.), Climate system modeling, Cambridge University Press, 1992, pp. 241–277.

[11] Sabine, C., Feely, R., Gruber, N., Key, R., Lee, K., Bullister, J., Wanninkhof, R., Wong, C., Peng, T., Kozyr, A., Ono, T., and Rios, A., The oceanic sink for anthropogenic CO_2, Science 305 (2004) 367–371.

[12] Sarmiento, J. L., and Gruber, N., Ocean Biogeochemical Dynamics, Princeton University Press, 2006.

[13] Seierstad, A., and Sydsæter, K., Optimal Control Theory with Economic Appliations, Advanced Textbooks in Economics, Elsevier Science Publishers B.V., Amsterdam, 1987.

[14] Tahvonen, O., Fossil fuels, stock externalities, and backstop technologies, Canad. J. Econom. 30, 4a (1997) 855–874.

[15] Tahvonen, O., and Withagen, C., Optimality of irreversible pollution accumulation, J. Econom. Dynam. Control 20 (1996) 1775–1795.

[16] Toman, M. A., and Withagen, C., Accumulative pollution, clean technology, and policy design, Resource and Energy Economics 22 (2000) 367–384.

5 Appendix

5.1 Paths for ψ, π, and $\psi - \pi$

We state that the paths for ψ, π, and $\lambda = \psi - \pi$ are either monotonically increasing or U-shaped when it is optimal to take action at all. Therefore, we have to show that the paths for ψ and π cannot have a maximum. In order to rule out this case, we use a line of argumentation similar to [14] and [4]. First, we show that ψ cannot have a maximum, second, we extend this result for π and λ, and third, we analyze the possible combinations of the two possible paths for the taxes.

Path for ψ: We consider the situation where ψ would have a maximum. At that point in time q would have a minimum, but would increase thereafter. The steady-state value for q is zero. Therefore, another point in time must emerge when ψ would reverse its sign and increase again. As a result, there would be two points in time, t_1 and t_2, when $\dot{\psi}_{t_1} = 0, \quad \ddot{\psi}_{t_1} < 0$, and $\dot{\psi}_{t_2} = 0, \quad \ddot{\psi}_{t_2} > 0$ must be valid. From the equation of motion for ψ, it follows that

$$\ddot{\psi}_{t_1} = -\gamma\dot{\pi} - D''_S\dot{S} < 0 \quad \text{and} \quad \ddot{\psi}_{t_2} = -\gamma\dot{\pi} - D''_S\dot{S} > 0 \tag{42}$$

would have to be fulfilled in order to reach a maximum for ψ at t_1 and a minimum at t_2. To determine the sign of the right-hand side of this equation, we have to distinguish four different cases at both points in time. The cases vary in the sign of $\dot{\pi}$, the sign of $\dot{S}$, and their absolute sizes at the

two points in time:

$$\begin{array}{llll} t_1 - Case1 & \dot{\pi} > 0, \dot{S} > 0, & t_2 - Case1 & \dot{\pi} < 0, \dot{S} < 0, \\ t_1 - Case2 & \dot{\pi} > 0, \dot{S} < 0 \quad |\dot{\pi}\gamma| > |D''_S \dot{S}|, & t_2 - Case2 & \dot{\pi} < 0, \dot{S} > 0 \quad |\dot{\pi}\gamma| > |D''_S \dot{S}|, \\ t_1 - Case3 & \dot{\pi} < 0, \dot{S} > 0 \quad |\dot{\pi}\gamma| < |D''_S \dot{S}|, & t_2 - Case3 & \dot{\pi} > 0, \dot{S} < 0 \quad |\dot{\pi}\gamma| < |D''_S \dot{S}|, \\ t_1 - Case4 & \dot{\pi} < 0, \dot{S} < 0, & t_2 - Case4 & \dot{\pi} > 0, \dot{S} > 0. \end{array} \tag{43}$$

First, we determine which combination of these cases can occur and which of them is in accordance with a maximum of ψ at t_1 and a minimum of ψ at t_2. Obviously, any inclusion of the case 4 at the two points in time would directly violate the necessary conditions (42). We can also exclude any combination where π is decreasing at both points in time, because we assume that ψ has a maximum at t_1 and a minimum at t_2. ψ is therefore monotonically decreasing between these two points in time, but increasing again thereafter. When π is still decreasing at point t_2, it would continue to decrease, as ψ increases thereafter. Therefore, the transversality condition for π would be violated. But a combination where π is increasing at point t_1 and decreasing at point t_2 can also be excluded. For this to happen, π would have a maximum between t_1 and t_2. The corresponding necessary condition therefore is that $\ddot{\pi} = -\gamma\omega\dot{\psi} < 0$. But for the considered combination, ψ is constantly decreasing between these two points in time. Therefore, the necessary condition for π to have a maximum is not fulfilled. As a result, we only have to consider combinations where π is either monotonically increasing or has a minimum. But if we observe case 2 at t_1 and case 3 at t_2, π is constantly increasing and S is monotonically decreasing. But this combination, which allows for a maximum of ψ at t_1 and a minimum of ψ at t_2, is only feasible if it is true that $|\dot{\pi}\gamma| > |D''_S \dot{S}|$ at t_1 and $|\dot{\pi}\gamma| < |D''_S \dot{S}|$ at t_2. However, as ψ is monotonically decreasing between these two points, whereby q is monotonically increasing, $\dot{\pi}$ increases towards to t_2, whereas the absolute size of $\dot{S}$ slows down given that it is decreasing at both points in time. Therefore, the sign of the inequality condition cannot reverse. This means that S has to have a maximum between t_1 and t_2 and π is either constantly increasing or has a minimum, which means in turn that we only have to consider case 1 or 3 at point t_1 and case 3 at point t_2. For S to reach a maximum, $\dot{S}$ must change signs between t_1 and t_2. Therefore, an intermediary point, $\tilde{t}$, must emerge where S has its maximum. We now determine in a second step whether these two remaining combinations are feasible for the various regimes implied by the distinction between the various Kuhn-Tucker conditions in Section 3.3. For the general case in Section 3.2 the investigation of Regime 1 applies.

Regime 1: In order to observe a maximum for S in Regime 1, the necessary condition to be fulfilled is $\ddot{S} = \dot{q} - \dot{a} + \gamma\omega\dot{W} < 0$ between t_1 and t_2. Given case 1 at t_1, q is increasing and a is decreasing. As a result, W must decrease for the necessary condition to be fulfilled. However, W can only decrease

when there is a net transfer from the lower box to the upper box and when the net transfer also exceeds the amount of sequestration. We know that the difference between q and a is increasing towards t_2, whereas case 3 states that S is decreasing. This is only possible if the net transfer into the lower box is positive. Therefore, W must have a minimum between $\tilde{t}$ and t_2, which implies $\ddot{W} = \dot{a} + \gamma\dot{S} > 0$. The last condition is a contradiction, as both a and S are decreasing for the combination of case 1 at t_1 and case 3 at t_2. In the other combination, namely case 3 at t_1 and case 3 at t_2, π has a minimum between t_1 and t_2. Therefore, we cannot necessarily state, that a is decreasing, because it could be the case that π is decreasing faster than ψ and therefore a increases. But when a increases, the tax difference $\lambda = \psi - \pi$ must have a maximum, as π has a minimum. For the tax difference λ to have a maximum, it must hold that $\ddot{\lambda} = -D''_S\dot{S} < 0$. As a consequence, S must be increasing, which in turn implies that at the maximum of S, a is already decreasing again, therefore the maximum condition would be violated and these two conditions cannot be both fulfilled simultaneously.

Regime 2: In order to observe a maximum for S in regime 2, the necessary condition to be fulfilled is $\ddot{S} = \dot{q} + \gamma\omega\dot{W} < 0$ between t_1 and t_2. Note that q is assumed to increase between t_1 and t_2. Therefore, $\gamma\omega\dot{W}$ must be negative and greater in absolute terms than $\dot{q}$. In order to see a decrease in the carbon stock in the lower box, W must have increased and had a maximum before $\tilde{t}$, because by assumption we have excluded situations where the initial level of S_0 is low and the initial level of W_0 is high. For W to reach a maximum before $\tilde{t}$, it must hold true that $\ddot{W} = \gamma\dot{S} < 0$. However, S is still increasing at that point in time ($\dot{S} > 0$), which contradicts the assumption for first W and then S to have a maximum.

Regime 3: In order to observe a maximum for S in regime 3, the necessary condition to be fulfilled is $\ddot{S} = \gamma\omega\dot{W} < 0$ between t_1 and t_2. The upper box, S, varies only in its size through the natural transfer of carbon with the lower box. In order to see a maximum for S, the net transfer of carbon from the lower box to the upper box has to be first positive but then negative. The switching point from a positive transfer towards a negative transfer corresponds to the maximum point of S. After this point in time, S becomes decreasing and W becomes increasing. If W was increasing before, the sufficient condition for a maximum of S is violated: $\ddot{S} = \omega\gamma\dot{W} < 0$. If W was decreasing before, the potential maximum point of S describes a situation where S and W are in equilibrium because the transfer rate will be zero. But thereafter S has to decrease, which is only possible, if W is relatively lower than S. But as we do not allow sequestration to be negative, this situation cannot occur after a point in time, when both carbon stocks have already achieved an equilibrium point. Therefore, we can also rule out that S has a maximum in this regime, regardless of whether the path of sequestration is constantly decreasing or has a maximum.

To sum up, we have shown that in all 3 regimes, the two remaining combinations are not feasible. Therefore, we rule out the possibility that ψ has a maximum. As a consequence, we can state that ψ will be either U-shaped or is monotonically increasing.

Path of π: Based on this conclusion we can extend the proposition to the path of π. When ψ can have only one extreme point, π cannot reverse its sign twice. Additionally, it is not possible for the path of π to approach its steady state value from above. Such a path would imply that π is decreasing, whereas ψ is increasing. As a consequence, π could not achieve a steady state, as it would continue to decrease. The steady state assumption and the transversality condition would be violated. Consequently, we rule out the possibility that π has a maximum and, thus, we state that π is either U-shaped or constantly increasing.

Path of λ: We extend the proposition for the tax difference, $\lambda = \psi - \pi$ based on the result that ψ and π are either monotonically increasing or U-shaped. When λ has an extremum, it must hold true that $\dot{\lambda} = \dot{\psi} - \dot{\pi} = 0$. Consequently, either both ψ and π are increasing or decreasing. When both ψ and π are monotonically increasing, which implies that S is monotonically increasing as well, it must hold true that $\dot{\psi} > \dot{\pi}$ the whole time, otherwise the transversality conditions would be violated. Additionally, a maximum for λ would imply that $\pi - \psi$ has a minimum. After λ_{max} has occured, $\dot{\pi}$ would be monotonically increasing and the transversality conditions would be violated. Therefore, the maximum of λ must be followed by a minimum of λ. A minimum requires $\ddot{\lambda} = -D''(S)\dot{S} > 0$, which can only be fulfilled when S decreases. But for ψ and π to be monotonically increasing, S has to increase monotonically as well. We state that λ has neither a maximum nor a minimum when ψ and π are monotonically increasing. When ψ and π are U-shaped, λ can have an extremum when both are still decreasing or when both are increasing again. A maximum for λ, while ψ and π are decreasing, implies that π decreases faster than ψ for some time and that we observe a maximum for λ at t_1, a minimum for π at t_2, and a minimum for ψ at t_3. Note, that for the U-shaped case, π has to reach its minimum before ψ, otherwise the sufficient condition $\ddot{\pi} = -\gamma\omega\dot{\psi} > 0$ would be violated. At t_1, the maximum of λ requires $\dot{S} > 0$ by $\ddot{\lambda} = -D''(S)\dot{S} < 0$, whereas at t_3 the minimum of ψ requires $\dot{S} < 0$ by $\ddot{\psi} = -\gamma\dot{\pi} - D''(S)\dot{S}$. As a consequence, S must have a maximum between t_1 and t_3 with the necessary condition $\ddot{S} = \dot{q} - \dot{a} + \gamma\omega W < 0$. λ and ψ are decreasing between t_1 and t_3. As a consequence, q is increasing, a is decreasing, and, therefore, W must be decreasing with $|\gamma\omega\dot{W}| > |\dot{q} - \dot{a}|$. S is decreasing after reaching its maximum, which requires W to increase, because our two-box model does not allow the carbon stocks in both boxes to decrease. Thereby, W must have a minimum at that point where S has a maximum when W is supposed to decrease before this point. But with both $\dot{W} = \dot{S} = 0$, the sufficient conditions for the maximum and the minimum are violated. As result, λ cannot have a maximum until ψ and π have passed their minima. Note that at

the minimum of π, it holds true that $\dot{\pi} = 0$ and $\dot{\psi} < 0$, which implies that λ has to be decreasing as well. After the two minima of ψ and π, both are monotonically increasing. Therefore, the previous argumentation where both are monotonically increasing the whole time applies again. We state that λ cannot have not a maximum when ψ and π are U-shaped, but must have a minimum.

Path combinations: The properties of the tax difference when ψ and π do not have a similar path remain to be investigated. When π is U-shaped, ψ has to be U-shaped as well in order to fulfill the sufficient condition for the minimum of π. But when ψ is U-shaped, it is not necessarily the case that π is U-shaped as well. We cannot rule out the possibility that π might also be monotonically increasing, even if this case never occurred when we parameterized the model and calculated paths for various initial conditions. Nevertheless, when ψ is U-shaped, there occurs a point in time when $\dot{\psi} = 0$ holds true, whereas π is monotonically increasing at that point in time, which implies that $\dot{\pi} > 0$. As a result, $\dot{\lambda} < 0$ which implies that λ will be U-shaped like ψ. The minimum of λ has to be at a later point in time than the minimum of ψ so that the argumentation used to show that λ cannot have a maximum is not affected by this special case.

5.2 Canonical System for Regimes 1 to 4

regime 1: The canonical system for Regime 1 is

$$\begin{pmatrix} \dot{\psi} \\ \dot{\pi} \\ \dot{S} \\ \dot{W} \end{pmatrix} = \begin{pmatrix} \rho+\gamma & -\gamma & -2s^2v_1 & 0 \\ -\gamma\omega & \gamma\omega+\rho & 0 & 0 \\ -\frac{a+u_2}{2u_2a_2} & \frac{1}{2a_2} & -\gamma & \gamma\omega \\ \frac{1}{2a_2} & -\frac{1}{2a_2} & \gamma & -\gamma\omega \end{pmatrix} \cdot \begin{pmatrix} \psi \\ \pi \\ S \\ W \end{pmatrix} + \begin{pmatrix} 2v_1sA_{preind} \\ 0 \\ \frac{a_1}{2a_2} + \frac{b}{2u_2} \\ -\frac{a_1}{2a_2} \end{pmatrix}, \tag{44}$$

with the corresponding steady state values

$$\psi_{ssr1} = b, \tag{45}$$

$$\pi_{ssr1} = \frac{b\gamma\omega}{\rho+\gamma\omega}, \tag{46}$$

$$S_{ssr1} = \frac{2sA_{preind}v_1(\rho+\gamma\omega) + b\rho(\gamma+\rho+\gamma\omega)}{2s^2v_1(\rho+\gamma\omega)}, \tag{47}$$

$$W_{ssr1} = \frac{-a_1s^2v_1(\rho+\gamma\omega) + 2a_2sA_{preind}v_1\gamma(\rho+\gamma\omega) + b\rho(s^2v_1 + a_2\gamma(\gamma+\rho+\gamma\omega))}{2a_2s^2v_1\gamma\omega(\rho+\gamma\omega)}. \tag{48}$$

The steady state values, S_{ssr1} and W_{ssr1} do not just differ by ω in the denominator. The steady state condition $(S - \omega W) = 0$ is violated. The dynamic system of Regime 1 does not converge to an admissible unique steady state.

Regime 2: The canonical system for Regime 2 is

$$\begin{pmatrix} \dot{\psi} \\ \dot{\pi} \\ \dot{S} \\ \dot{W} \end{pmatrix} = \begin{pmatrix} \rho+\gamma & -\gamma & -2s^2v_1 & 0 \\ -\gamma\omega & \gamma\omega+\rho & 0 & 0 \\ -\frac{1}{2u_2} & 0 & -\gamma & \gamma\omega \\ 0 & 0 & \gamma & -\gamma\omega \end{pmatrix} \cdot \begin{pmatrix} \psi \\ \pi \\ S \\ W \end{pmatrix} + \begin{pmatrix} 2v_1sA_{preind} \\ 0 \\ \frac{b}{2u_2} \\ 0 \end{pmatrix}, \tag{49}$$

with the corresponding steady state values

$$\begin{aligned} \psi_{ssr2} &= b, && (50)\\ \pi_{ssr2} &= \frac{b\gamma\omega}{\rho+\gamma\omega}, && (51)\\ S_{ssr2} &= \frac{2sA_{preind}v_1(\rho+\gamma\omega)+b\rho(\gamma+\rho+\gamma\omega)}{2s^2v_1(\rho+\gamma\omega)}, && (52)\\ W_{ssr2} &= \frac{2sA_{preind}v_1(\rho+\gamma\omega)+b\rho(\gamma+\rho+\gamma\omega)}{2s^2v_1\omega(\rho+\gamma\omega)}. && (53) \end{aligned}$$

The steady state values, S_{ssr2} and W_{ssr2}, differ only by ω in the denominator of W_{ssr2}. The steady state condition $(S-\omega W)=0$ is fulfilled. FOC (22) for the determination of a is fulfilled, with either $a_1 = a_{crit}$ and $\theta_2 = 0$ or $a_1 > a_{crit}$ and $\theta_2 > 0$. For both combinations, the dynamic system converges to a unique steady state that is characterized by low steady state values.

Regime 3: The canonical system for Regime 3 is

$$\begin{pmatrix} \dot{\psi} \\ \dot{\pi} \\ \dot{S} \\ \dot{W} \end{pmatrix} = \begin{pmatrix} \rho+\gamma & -\gamma & -2s^2v_1 & 0 \\ -\gamma\omega & \gamma\omega+\rho & 0 & 0 \\ 0 & 0 & -\gamma & \gamma\omega \\ 0 & -\frac{1}{2(u_2+a_2)} & \gamma & -\gamma\omega \end{pmatrix} \cdot \begin{pmatrix} \psi \\ \pi \\ S \\ W \end{pmatrix} + \begin{pmatrix} 2v_1sA_{preind} \\ 0 \\ 0 \\ \frac{b-a_1}{2(u_2+a_2)} \end{pmatrix}, \tag{54}$$

with the corresponding steady state values

$$\begin{aligned} \psi_{ssr3} &= \frac{(b-a_1)(\gamma\omega)+\rho}{\gamma\omega}, && (55)\\ \pi_{ssr3} &= b-a_1, && (56)\\ S_{ssr3} &= \frac{2sA_{preind}v_1\gamma\omega - a_1\rho(\gamma+\rho+\gamma\omega)+b\rho(\gamma+\rho+\gamma\omega)}{2s^2v1\gamma\omega}, && (57)\\ W_{ssr3} &= \frac{2sA_{preind}v_1\gamma\omega - a_1\rho(\gamma+\rho+\gamma\omega)+b\rho(\gamma+\rho+\gamma\omega)}{2s^2v_1\gamma\omega^2}. && (58) \end{aligned}$$

The steady state values, S_{ssr3} and W_{ssr3}, differ only by ω in the denominator of W_{ssr3}. The steady state condition $(S-\omega W)=0$ is fulfilled. FOCs (21) and (22) for the determination of q and a simplify to $q = a = \frac{b-a_1-\pi}{2(u_2+a_2)}$, which is fulfilled for the steady state values ψ_{ssr3} and π_{ssr3}. The dynamic system

converges to a unique steady state that is characterized by large steady state values. The steady state values for S in Regime 3 differ from those Regime 1 by $S_{ssr3} - S_{ssr1} = \frac{\rho(\gamma+\rho+\gamma\omega)(b\rho - a_1(\rho+\gamma\omega))}{2s^2 v_1 \gamma\omega(\rho+\gamma\omega)}$. The difference is positive when $a_1 < a_{crit}$, which is the condition for the steady state of Regime 3 to emerge.

Regime 4: The canonical system for Regime 4 is

$$\begin{pmatrix} \dot{\psi} \\ \dot{\pi} \\ \dot{S} \\ \dot{W} \end{pmatrix} = \begin{pmatrix} \rho+\gamma & -\gamma & -2s^2 v_1 & 0 \\ -\gamma\omega & \gamma\omega+\rho & 0 & 0 \\ 0 & 0 & -\gamma & \gamma\omega \\ 0 & 0 & \gamma & -\gamma\omega \end{pmatrix} \cdot \begin{pmatrix} \psi \\ \pi \\ S \\ W \end{pmatrix} + \begin{pmatrix} 2v_1 s A_{preind} \\ 0 \\ 0 \\ 0 \end{pmatrix}, \tag{59}$$

with the corresponding steady state values

$$\psi_{ssr4} = \frac{2sv_1(\rho+\gamma\omega)(-A_{pred} + \frac{s(S_0+W_0)\omega}{1+\omega}}{\rho(\gamma+\rho+\gamma\omega)}, \tag{60}$$

$$\pi_{ssr4} = \frac{2sv_1\gamma\omega(-A_{pred} + \frac{s(S_0+W_0)\omega}{1+\omega}}{\rho(\gamma+\rho+\gamma\omega)}, \tag{61}$$

$$S_{ssr4} = \frac{\omega(S_0+W_0)}{1+\omega}, \tag{62}$$

$$W_{ssr4} = \frac{S_0+W_0}{1+\omega}. \tag{63}$$

The steady state values, S_{ssr4} and W_{ssr4} ,differ only by ω in the denominator of W_{ssr4}. The steady state condition $(S - \omega W) = 0$ is fulfilled. FOCs (21) and (22) for the determination of q and a are fulfilled with $a_1 \lessgtr a_{crit}$ but with $\theta_1 > 0$ and $\theta_2 > 0$. The steady state values are greater than the specific steady state values for the given level of a_1 in Regime 2 or Regime 3.

5.3 Stability Analysis for Regime 2, Regime 3, and Regime 4

Regime 2: In order to show the saddle path properties of Regime 2, we calculate the eigenvalues of the system using theorem 1 of Dockner [3] p. 94:

$$p_{1,2,3,4} = \frac{\rho}{2} \pm [(\frac{\rho}{2})^2 - \frac{K}{2} \pm \frac{1}{2}(K^2 - 4 * \mathrm{Det}(J))^{0.5}]^{0.5}, \tag{64}$$

where J is the Jacobian of the dynamic system and K is due to Dockner [3] p. 100:

$$K = -\frac{s^2 v_1 + u2\gamma(1+\omega)(\gamma+\rho+\gamma\omega)}{u_2}, \quad \mathrm{Det}(J) = \frac{s^2 v_1 \gamma\omega(\rho+\gamma\omega)}{u_2}. \tag{65}$$

The two necessary and sufficient conditions for the eigenvalues (64) to be real, with two of the eigenvalues being positive and two being negative are due to theorem 3 of Dockner [3] p.96 are

$$K < 0 \quad \text{and} \quad 0 < \text{Det}(J) \leq \frac{K^2}{4}. \tag{66}$$

The determinant of Regime 2 is positive and K is obviously below zero. The last condition is fulfilled if

$$(s^2 v_1 + u_2 \gamma(1+\omega)(\gamma + \rho + \gamma\omega))^2 \geq 4 s^2 u_2 v_1 \gamma\omega(\rho + \gamma\omega). \tag{67}$$

Given that condition (67) is fulfilled, the dynamic system in Regime 2 obeys saddle path properties.
Regime 3: The proof for Regime 3 follows the same line of argumentation, whereby the values for J, the determinant of the Jacobian in Regime 3, and K are

$$\text{Det(J)} = \frac{s^2 v_1 \gamma^2 \omega^2}{a_2 + u_2}, \quad K = -\gamma(1+\omega)(\gamma + \rho + \gamma\omega). \tag{68}$$

The determinant of Regime 3 is positive and K is obviously below zero. The condition $0 <$Det(J)$\leq \frac{K^2}{4}$ is fulfilled if

$$(1+\omega)^2(\gamma + \rho + \gamma\omega)^2 \geq (4 s^2 v_1 \omega^2)/(a_2 + u_2). \tag{69}$$

Given that condition (69) is fulfilled, the dynamic system in Regime 3 obeys saddle path properties.
Regime 4: The simple canonical system for Regime 4 allows to calculate directly the eigenvalues, which turn out to be

$$p_1 = 0, \quad p_2 = \rho, \quad p_3 = -\gamma - \gamma\omega, \quad p_4 = \gamma + \rho + \gamma\omega. \tag{70}$$

We can choose the initial values of the two taxes, ψ and π, in accordance with the initial values of the state variables, S_0 and W_0, so that the constants associated with the positive eigenvalues become zero. The dynamic system is then stable.